

Real Time Implementation of Successive Radon Transformation for Electrical Impedance Tomography

Aamin Ridibeh, Misaddy Hoche

Assistant Professor, University of Kalyani, India

Article Information

Received : 02 Sept 2024
Revised : 06 Sept 2024
Accepted : 18 Sept 2024
Published : 22 Sept 2024

Corresponding Author:

G. Me

Abstract— This paper Radon Transformation is generally used to construct optical image (like CT image) from the projection data in biomedical imaging. In this paper, the concept of Radon Transformation is implemented to reconstruct Electrical Impedance Topographic Image (conductivity or resistivity distribution) of a circular subject. A parallel resistance model of a subject is proposed for Electrical Impedance Topography(EIT) or Magnetic Induction Tomography(MIT). A circular subject with embedded circular objects is segmented into equal width slices from different angles. For each angle, Conductance and Conductivity of each slice is calculated and stored in an array. A back projection method is used to generate a two-dimensional image from one-dimensional projections. As a back projection method, Inverse Radon Transformation is applied on the calculated conductance and conductivity to reconstruct two dimensional images. These images are compared to the target image. In the time of image reconstruction, different filters are used and these images are compared with each other and target image.

Keywords: Biomedical imaging, EIT, MIT, Radon Transformation, Inverse Radon Transformation

Copyright © 2024: Aamin Ridibeh, Misaddy Hoche, This is an open access distribution, and reproduction in any medium, provided Access article distributed under the Creative Commons Attribution License the original work is properly cited License, which permits unrestricted use.

Citation: Aamin Ridibeh, Misaddy Hoche, “Real Time Implementation of Successive Radon Transformation for Electrical Impedance Tomography”, Journal of Science, Computing and Engineering Research, 7(9), September 2024.

I. INTRODUCTION

Medical imaging is the technique used to create images of the human body (or parts and function thereof) for clinical purposes (medical procedures seeking to reveal, diagnose or examine disease) or medical science (including the study of normal anatomy and physiology). Image of internal structure of a body is definitely a useful tool for diagnosis, treatment and biomedical research. Soon after the discovery of X-rays, their importance as a tool for biomedical diagnosis was recognized and X-ray machine became the first widely used electrical instrument in medicine. However, X-ray causes tissue damage in the body and cannot be used for long time monitoring [1]. In the past three decades, we have noticed tremendous developments in this field; new techniques include X-ray computed tomography (CT), magnetic resonance imaging (MRI), ultrasound imaging, positron emission tomography (PET), and so on. Each of these imaging modalities provides a particular functionality or certain unique features that cannot be replaced by tomography (CT) imaging and MRI. X-ray CT imaging has a good resolution; however, it may damage the tissue. MRI also has a good resolution and it does not cause any tissue damage. The instrument, however, is very expensive and too large in size to be used in normal patients' bedrooms in a hospital. The advantages of ultrasound imaging include bedside availability and the relative ease of performing repeated examinations. Imaging is real-time and free of harmful radiation. There are no documented side effects and discomfort is minimal [2]. The

disadvantages of ultrasonography are primarily related to the fact that it is heavily operator-dependent. Retrospective review of images provides only limited quality control. There is no scout scan to give a global picture for orientation [2]. Electric impedance imaging is a method of reconstructing the internal impedance distribution of a human body based on the measurements from the outside. A very low-level current requirement gives it the advantage of having no biological hazard and allows long-term monitoring for the intensive care of patients. Therefore, this method is expected to be a very efficient and useful method in the biomedical field [1]. Much research has been done and significant efforts are still being made toward the realization of electrical imaging. One common method known as electrical impedance tomography (EIT) is promising. But it involves the challenge of attaching a large number of electrodes to the body surface [3]–[5]. Another method involving magnetic excitation with coils and measurements of surface potential with electrodes has been proposed [6],[7]. In this method, however, the measurement sensitivity at the centre region is much less than that obtained in the peripheral regions. In the last decade, many studies have reported on a similar method known as magnetic induction tomography (MIT) [8]–[16]. In MIT, a magnetic field is applied from an array of excitation coils to induce eddy currents in the body, and the magnetic field from these currents is then detected using a separate set of sensing coils. The great advantage of MIT in contrast to EIT is the contactless operation, so that the positioning of the

electrodes and the ill-defined electrode skin interface can be avoided [9]. However, the sensitivity of this method is not uniform over the measurement area [9]. Another difficulty encountered with this method is that the excitation field also induces a signal in the sensing coil, and the signal due to the eddy current in the material is normally much smaller in comparison [10]. In order to overcome this difficulty, various methods have been devised [9],[11]. However, there still remain some significant drawbacks [11]. For example, using a planar gradiometer arrangement, a ghost object can be recognized in the reconstructed image [15]. In some cases, to reconstruct the image from measurement data, a weighted back projection method has been proposed [16]. Unfortunately, the weights have been calculated only in the case of conducting perturbations in empty space, which is quite different from anatomical structures [12]. In this research work a back projection method based on Inverse Radon Transformation is proposed to reconstruct 2D image of conductivity or resistivity distribution. A circular subject with embedded circular objects is taken and segmented into equal width slices from different angles. For each angle, Conductance and Conductivity of each slice is calculated and stored in an array. Inverse Radon Transformation is used to generate a two dimensional image (Reconstructed image) from one-dimensional projections (conductivity or resistivity distribution). This Reconstructed image is compared to the target image. Different types of filters with different interpolations are used in image reconstruction process and these images are compared with each other and target image.

METHODS

In this research work, circular subjects of different sizes are taken as models. One or more small circular perturbation embedded within the circular subject as shown in Figure 1.a. The resistivity of circular subject and the embedded perturbation are known. To calculate projection of conductivity distribution at a particular angle, the subject is sliced into number of segments shown in figure 1.b where projections values for each slice is taken from 1350 angle. Figure 1.C shows, Subject is sliced into number of segments and projections values for each slice is taken from 900 angles. Average conductance and conductivity of each slice is calculated as projection value. In the similar way, the circular subject is segmented from different angles. For each angle, Conductivities and Conductance's of all slices are calculated. Thus we find the projection values of conductances and conductivities of the subject for each angle. For example, if the circular subject is divided into N slices. The circular subject is rotated by θ_i angle ($\theta_i = 1, 2, 3, 4, \dots, 180$). Then total number of rotation is $R_i = 180/\theta_i$. For each rotational angle Q_c ($Q_c = \theta_i, \theta_i + \theta_i, \dots, 180$) Conductance and Conductivity of N slices are calculated. Calculated Conductance is $Conductanc[N][R_i]$ & Conductivity is $Conductivity[N][R_i]$. To calculate

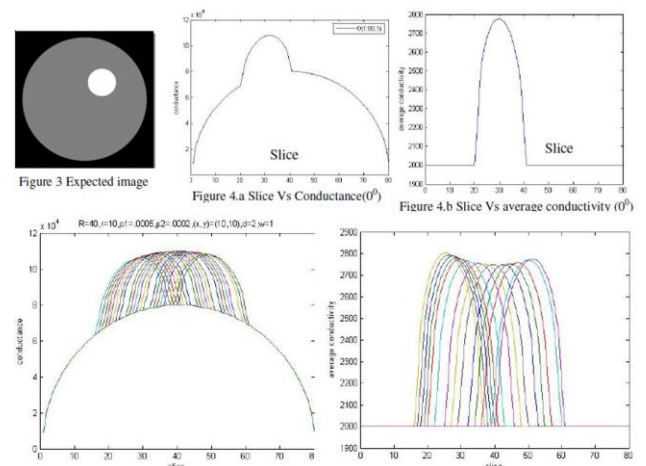
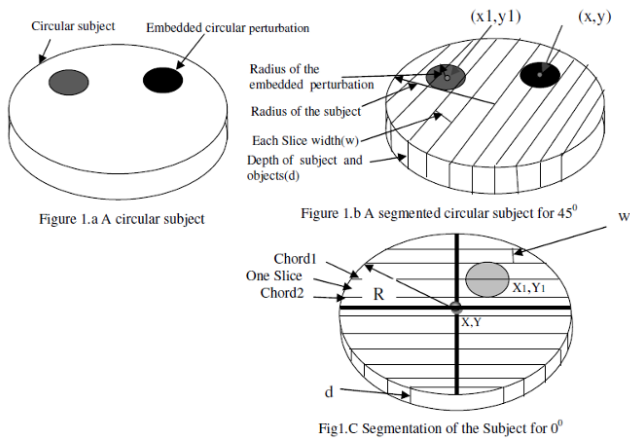
conductivity and conductance, each slice average length is calculated. Lengths of chords are calculated using the following formula $Chord = 2 * (\text{where } i = \text{Radius} - w_i, w \text{ is the wide of each slice } w_i = 0, w, 2w, 3w, \dots, \text{Radius})$. Each slice has two chords. Using these two chords, average length is calculated. Using following equations, conductance and average conductivity are calculated. We know conductance or $\sigma =$

.....(1)
Conductivity or Average conductivity = $A = \text{average length of slice} * W$ 1 is the depth of the circular subject. is the resistivity of object or subject. International Journal of Information Sciences and Techniques (IJIST) Vol.2, No.5, September 2012 14 If the axes of circular subject(centre fixed) is rotated about an angle θ_i , then centre of the perturbation is calculated for the new axes using following equations $X = x_1 * \cos Q_c + y_1 * \sin Q_c$;

.....(2)
 $Y = -x_1 * \sin Q_c + y_1 * \cos Q_c$;

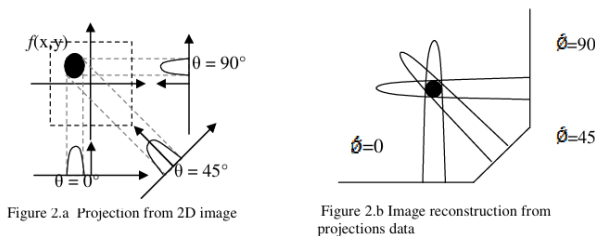
.....(3)
Where (x_1, y_1) is the perturbation centre for old axes and (X, Y) is the perturbation centre of that perturbation for new axes. In each slice, one or more embedded perturbations segments can have or not. So general equation for calculating conductance for each slice is $Conductance = + + + \dots + \dots + \dots$ (4) Where

$L_{cbcs1} = \text{chord1} - (C_1 + C_3 + \dots + C_{n-1})$ (chord1 is one slice upper chord of the subject and c_1, c_3, \dots, c_{n-1} are chords of embedded perturbations circle1, circle2, circle_n . The Values of c_1, c_3, \dots, c_{n-1} can be zero or can have value depending on whether embedded perturbations chords are included with chord1 or not included with chord1) $L_{cbcs2} = \text{chord2} - (C_2 + C_4 + \dots + C_n)$ (chord2 is one slice another chord of the subject and c_2, c_4, \dots, c_n are chords of embedded perturbations circle1, circle2, circle_n . The Values of c_2, c_4, \dots, c_n can be zero or can have value depending on whether embedded perturbations chords are included with chord1 or not included with chord2) $L_{nc} =$ (average length of one slice of the subject without the segments of embedded circular perturbations) $L_{nc1} =$ (average length of one slice of embedded circle1) $L_{nc2} =$ (average length of one slice of embedded circle2) $L_{ncn} =$ (average length of one slice of embedded circle_n) are the resistivities of subject, embedded circular perturbations circle1, circle2, circle_n respectively. $Conductanc[N][R_i]$ are One-dimensional projections data taken from different angles using conductance of each slice and $Conductivity[N][R_i]$ are One-dimensional projections data taken from different angles using conductivity of each slice. The 2D Radon transformation is the projection of the image intensity along a radial line oriented at a specific angle. The general equation of the Radon transformation is acquired [17]–[21] $\int\int - + \cdot = dx dy s y x y x f s g) \sin \cos () , () , (\theta \theta \delta \theta$ (5)



To reconstruct the image from one-dimensional projections data from different angles, the Inverse Radon Transform is applied to the one-dimensional projections data. The inverse of Radon transform is calculated by the following equation [22] :

.....(6)
 where θ is the Radon transformation, ρ is a filter and (θ) is the angle of the projection. To get $f(x,y)$ back, from equation (5) is known as inverse Radon transform. Figure 2.b shows the formation of image from the projections taken at angles 0° , 45° , and 90° that is shown in Figure 2.a.



EXPERIMENT AND RESULTS: One embedded circular perturbation in the Subject: We took Radius of the subject, $R=40\text{mm}$, embedded object $r_1=10\text{mm}$, resistivity of the subject, $p=0.0005\ \Omega\text{m}$, resistivity of the object $p_1=0.0002\ \Omega\text{m}$, Depth of the subject $d=2\text{mm}$ and slice wide $w=1\text{mm}$, rotational angle $q=100^\circ$ & centre of the embedded object $(x,y)=(10,10)$, then expected image is shown in Figure 3. slice Vs Conductance and slice Vs average conductivity are shown in Figure 4.a and Figure 4.b for 0° angle respectively and Figure 4.c & Figure 4.d for $0, 5, 10, \dots, 180^\circ$ degree angles respectively.

Figure 4 shows Slice Vs Conductance & Slice Vs average conductivity graph for different angles. Using Inverse Radon Transformation on the calculated average Conductivity and conductance for all angles image is obtained Shown in Fig 5.a & 5.b.



Figure 6 shows normalized average conductivity images, normalized conductance images & target images for $R=40\text{mm}$, $r_1=10\text{mm}$, $p_1=0.0005\ \Omega\text{m}$, $p_2=0.0002\ \Omega\text{m}$, $(x,y)=(-10,10)$, $w=1\text{mm}$, $d=2\text{mm}$, $q=10^\circ$ & $R=40\text{mm}$, $r_1=10\text{mm}$, $p_1=0.0005\ \Omega\text{m}$, $p_2=0.0002\ \Omega\text{m}$, $x=10$, $y=-10$, $w=1\text{mm}$, $d=2\text{mm}$, $q=10^\circ$. Two embedded perturbations in the Subject: we took Radius of the subject $R=40\text{mm}$, objects (perturbation) $r_1=8\text{mm}$, $r_2=12\text{mm}$, resistivity of subject $p_1=0.0005\ \Omega\text{m}$, resistivity of embedded objects $p_2=0.0002\ \Omega\text{m}$, $p_3=$

Depth of subject $d=2\text{mm}$ and slice wide $w=1\text{mm}$, rotational angle $q=5^\circ$ and centre of the embedded objects $(x,y)=(10,14)$, $(x_1,y_1)=(-12,-10)$, the expected image is shown in Figure 7. Slice Vs Conductance and slice Vs average Conductivity are shown in Figure 8.a. and Figure 8.b respectively for 0 (zero) degree angle and Figure 8.c & Figure 8.d for $0, 5, 10, \dots, 180^\circ$ degree angles respectively. Using Inverse Radon Transformation on the 1D calculated average Conductivity and conductance for all angles ($0, 5, 10, \dots, 180^\circ$) images are obtained as shown in Figure 9.

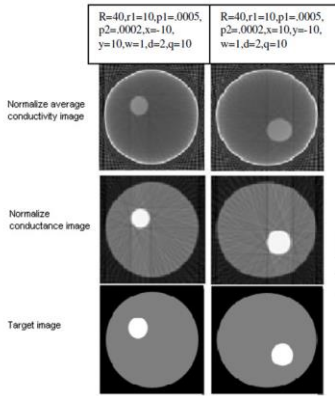


Figure 6. Normalize average conductivity, normalize conductance & target images for different positions of embedded circle

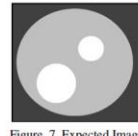


Figure 7 Expected Image

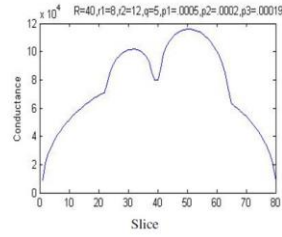


Figure 8.a Slice Vs Conductance (0°)

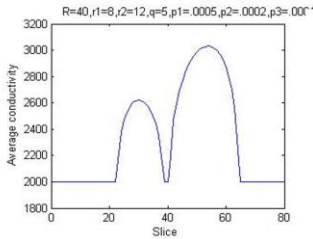


Figure 8.b Slice Vs average conductivity (0°)

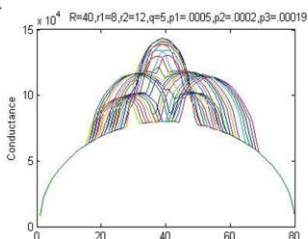


Figure 8.c Slice Vs conductance ($0^\circ, 5^\circ, 10^\circ, \dots, 180^\circ$)

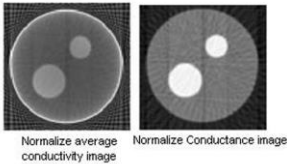


Figure 9. Normalize average conductivity & conductance images, where $R=40\text{mm}$, $r1=8\text{mm}$, $r2=12\text{mm}$, $p1=0.0005\ \Omega\text{m}$, $p2=0.0002\ \Omega\text{m}$, $p3=0.000199\ \Omega\text{m}$, $(x,y)=(10,14)$, $(x1,y1)=(-12,-10)$

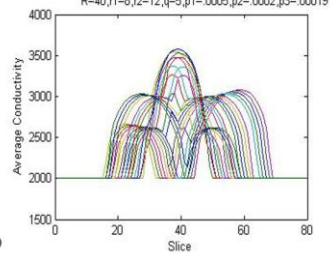


Figure 8.d Slice Vs average conductivity ($0^\circ, 5^\circ, 10^\circ, \dots, 180^\circ$)

We used radius and resistivity of the subject $R = 40\text{mm}$, $p1=.0005\ \Omega\text{m}$, for embedded perturbations, radius are $r1=10\text{mm}$, $r2=5\text{mm}$, & resistivity $p2=.008\ \Omega\text{m}$, $p3=.009\ \Omega\text{m}$ & centre positions are $(x,y)=(10,10)$, $(x1,y1)=(-8,8)$ respectively, slice width $w=1\text{mm}$, Depth of the subject and objects is $d=2$, rotational angle $q=5$, then obtained normalize and without normalize average conductivity and conductance images without any filters is shown in Figure-10.

Comparator is a circuit that output is binary information depending upon the comparison of two input voltages here the comparison in between analog voltage and reference voltage. Analog voltage is greater than reference voltage, and then comparator output is logic '1'. The comparator output is logic '0', when analog voltage is less than

reference voltage. Comparators are effectively used in analog to digital (ADC) converters. In analog to digital conversion process [1], the analog voltage is converted in to samples for getting accuracy. Those samples are given to set of comparators in order to achieve equivalent binary information. The schematic of

Hence, designing highspeed comparators with low supply voltages many techniques are there such boosting [6] methods, techniques employing body driven comparator circuit works in reset phase. CMOS technology

II. RELATED WORKS

In comparator circuits to reduce power consumption the Power gating technique is proposed. In this technique, circuit operates in sleep mode by switching off the current in circuit. Power gating has the benefit that is it measures current (I_{dd}) in the quiescent state. In this paper the different architectures of double tail comparator is presented. The proposed comparator is designed by using power gating technique. Using this technique power and delay is reduced.

III. BACKGROUND OF STUDY

The circuit diagram of the single tail comparator shown in Fig 3. The single tail comparator circuit operation is given below. When $\text{CLK}=0$ the circuit works in reset phase so the Mtail NMOS transistor is in off position and the reset transistors M7 and M8 PMOS transistors are in on position now the output at OUTN and OUTP will be VDD. When $\text{CLK}= \text{VDD}$, Mtail NMOS transistor is in ON position and M7 and M8 PMOS transistors are in OFF position now the OUTN and OUTP current to keep the differential amplifiers in weak condition so a large current required enabling fast regeneration in the circuit.

IV. CONCLUSION

In this thesis work, we have proposed a parallel resistance model for Electrical Impedance Imaging. With some simulation study, we have shown that this model can be used to reconstruct internal resistivity or conductivity or conductance distribution images. There are some differences in target image and reconstructed image. Different types of filters with different interpolations are used in image reconstruction process. But in the reconstructed images, no significant difference is observed. If the rotational angle is small then produced images are better. From the reconstructed images with different condition we can conclude that this model can be used for Electrical Impedance Tomography (EIT) or Magnetic Induction Tomography(MIT).

REFERENCES

- [1]. P. Nirmala, T. Manimegalai, J. R. Arunkumar, S. Vimala, G. Vinoth Rajkumar, Raja Raju, "A Mechanism for Detecting the Intruder in the Network through a Stacking Dilated CNN

- Model", *Wireless Communications and Mobile Computing*, vol. 2022, Article ID 1955009, 13 pages, 2022. <https://doi.org/10.1155/2022/1955009>.
- [2]. D. Sathyanarayanan, T. S. Reddy, A. Sathish, P. Geetha, J. R. Arunkumar and S. P. K. Deepak, "American Sign Language Recognition System for Numerical and Alphabets," 2023 International Conference on Research Methodologies in Knowledge Management, Artificial Intelligence and Telecommunication Engineering (RMKMATE), Chennai, India, 2023, pp. 1-6, doi: 10.1109/RMKMATE59243.2023.10369455.
- [3]. J. R. Arunkumar, Tägele berihun Mengist, 2020" Developing Ethiopian Yirgacheffe Coffee Grading Model using a Deep Learning Classifier" *International Journal of Innovative Technology and Exploring Engineering (IJITEE)* ISSN: 2278-3075, Volume-9 Issue-4, February 2020. DOI: 10.35940/ijitee.D1823.029420.
- [4]. Ashwini, S., Arunkumar, J.R., Prabu, R.T. et al. Diagnosis and multi-classification of lung diseases in CXR images using optimized deep convolutional neural network. *Soft Comput* (2023). <https://doi.org/10.1007/s00500-023-09480-3>
- [5]. J.R.Arunkumar, Dr.E.Muthukumar," A Novel Method to Improve AODV Protocol for WSN" in *Journal of Engineering Sciences* ISSN NO: 0377-9254 Volume 3, Issue 1, Jul 2012.
- [6]. R. K. A. Shameem, P. Biswas, B. T. Geetha, J. R. Arunkumar and P. K. Lakineni, "Supply Chain Management Using Blockchain: Opportunities, Challenges, and Future Directions," 2023 Second International Conference on Informatics (ICI), Noida, India, 2023, pp. 1-6, doi: 10.1109/ICI60088.2023.10421633.
- [7]. Arunkumar, J. R. "Study Analysis of Cloud Security Challenges and Issues in Cloud Computing Technologies." *Journal of Science, Computing and Engineering Research* 6.8 (2023): 06-10.
- [8]. J. R. Arunkumar, R. Raman, S. Sivakumar and R. Pavithra, "Wearable Devices for Patient Monitoring System using IoT," 2023 8th International Conference on Communication and Electronics Systems (ICCES), Coimbatore, India, 2023, pp. 381-385, doi: 10.1109/ICCES57224.2023.10192741.
- [9]. S. Sugumaran, C. Geetha, S. S. P. C. Bharath Kumar, T. D. Subha and J. R. Arunkumar, "Energy Efficient Routing Algorithm with Mobile Sink Assistance in Wireless Sensor Networks," 2023 International Conference on Advances in Computing, Communication and Applied Informatics (ACCAI), Chennai, India, 2023, pp. 1-7, doi: 10.1109/ACCAI58221.2023.10201142.
- [10]. R. S. Vignesh, V. Chinnammal, Gururaj.D, A. K. Kumar, K. V. Karthikeyan and J. R. Arunkumar, "Secured Data Access and Control Abilities Management over Cloud Environment using Novel Cryptographic Principles," 2023 International Conference on Advances in Computing, Communication and Applied Informatics (ACCAI), Chennai, India, 2023, pp. 1-8, doi: 10.1109/ACCAI58221.2023.10199616.
- [11]. Syamala, M., Anusuya, R., Sonkar, S.K. et al. Big data analytics for dynamic network slicing in 5G and beyond with dynamic user preferences. *Opt Quant Electron* 56, 61 (2024). <https://doi.org/10.1007/s11082-023-05663-2>
- [12]. Krishna Veni, S. R., and R. Anusuya. "Design and Study Analysis Automated Recognition system of Fake Currency Notes." *Journal of Science, Computing and Engineering Research* 6.6 (2023): 16-20.
- [13]. V. RamKumar, S. Shanthi, K. S. Kumar, S. Kanageswari, S. Mahalakshmi and R. Anusuya, "Internet of Things Assisted Remote Health and Safety Monitoring Scheme Using Intelligent Sensors," 2023 International Conference on Advances in Computing, Communication and Applied Informatics (ACCAI), Chennai, India, 2023, pp. 1-8, doi: 10.1109/ACCAI58221.2023.10199766.
- [14]. R. S. Vignesh, R. Sankar, A. Balaji, K. S. Kumar, V. Sharmila Bhargavi and R. Anusuya, "IoT Assisted Drunk and Drive People Identification to Avoid Accidents and Ensure Road Safety Measures," 2023 International Conference on Advances in Computing, Communication and Applied Informatics (ACCAI), Chennai, India, 2023, pp. 1-7, doi: 10.1109/ACCAI58221.2023.10200809.
- [15]. I. Chandra, G. Sowmiya, G. Charulatha, S. D, S. Gomathi and R. Anusuya, "An efficient Intelligent Systems for Low-Power Consumption Zigbee-Based Wearable Device for Voice Data Transmission," 2023 International Conference on Artificial Intelligence and Knowledge Discovery in Concurrent Engineering (ICECONF), Chennai, India, 2023, pp. 1-7, doi: 10.1109/ICECONF57129.2023.10083856.
- [16]. G. Karthikeyan, D. T. G, R. Anusuya, K. K. G, J. T and R. T. Prabu, "Real-Time Sidewalk Crack Identification and Classification based on Convolutional Neural Network using Thermal Images," 2022 International Conference on Automation, Computing and Renewable Systems (ICACRS), Pudukkottai, India, 2022, pp. 1266-1274, doi: 10.1109/ICACRS55517.2022.10029202.
- [17]. R. Meena, T. Kavitha, A. K. S, D. M. Mathew, R. Anusuya and G. Karthik, "Extracting Behavioral Characteristics of College Students Using Data Mining on Big Data," 2023 International Conference on Artificial Intelligence and Knowledge Discovery in Concurrent Engineering (ICECONF), Chennai, India, 2023, pp. 1-7, doi: 10.1109/ICECONF57129.2023.10084276.
- [18]. S. Bharathi, A. Balaji, D. Irene. J, C. Kalaivanan and R. Anusuya, "An Efficient Liver Disease Prediction based on Deep Convolutional Neural Network using Biopsy Images," 2022 3rd International Conference on Smart Electronics and Communication (ICOSEC), Trichy, India, 2022, pp. 1141-1147, doi: 10.1109/ICOSEC54921.2022.9951870.
- [19]. I. Chandra, G. Sowmiya, G. Charulatha, S. D, S. Gomathi and R. Anusuya, "An efficient Intelligent Systems for Low-Power Consumption Zigbee-Based Wearable Device for Voice Data Transmission," 2023 International Conference on Artificial Intelligence and Knowledge Discovery in Concurrent Engineering (ICECONF), Chennai, India, 2023, pp. 1-7, doi: 10.1109/ICECONF57129.2023.10083856.
- [20]. Revathi, S., et al. "Developing an Infant Monitoring System using IoT (INMOS)." *International Scientific Journal of Contemporary Research in Engineering Science and Management* 6.1 (2021): 111-115.
- [21]. J.R.Arunkumar, Dr.E.Muthukumar, A Novel Method to Improve AODV Protocol for WSN in *Journal of Engineering Sciences* ISSN NO: 0377-9254 Volume 3, Issue 1, Jul 2012.

- [22].R. S. Vignesh, A. Kumar S, T. M. Amirthalakshmi, P. Delphy, J. R. Arunkumar and S. Kamatchi, "An Efficient and Intelligent Systems for Internet of Things Based Health Observance System for Covid 19 Patients," 2023 International Conference on Artificial Intelligence and Knowledge Discovery in Concurrent Engineering (ICECONF), Chennai, India, 2023, pp. 1-8, doi: 10.1109/ICECONF57129.2023.10084066.
- [23].I. Chandra, K. V. Karthikeyan, R. V, S. K, M. Tamilselvi and J. R. Arunkumar, "A Robust and Efficient Computational Offloading and Task Scheduling Model in Mobile Cloud Computing," 2023 International Conference on Artificial Intelligence and Knowledge Discovery in Concurrent Engineering (ICECONF), Chennai, India, 2023, pp. 1-8, doi: 10.1109/ICECONF57129.2023.10084293.
- [24].R. K, A. Shameem, P. Biswas, B. T. Geetha, J. R. Arunkumar and P. K. Lakineni, "Supply Chain Management Using Blockchain: Opportunities, Challenges, and Future Directions," 2023 Second International Conference on Informatics (ICI), Noida, India, 2023, pp. 1-6, doi: 10.1109/ICI60088.2023.10421633.
- [25].J. R. Arunkumar, and R. Anusuya, "OCHRE: A Methodology for the Deployment of Sensor Networks." American Journal of Computing Research Repository, vol. 3, no. 1 (2015): 5-8.

